The Effects of Wind Veer During the Morning and Evening Transitions

M Sanchez Gomez[1], J K Lundquist[2,3]

[1]Department of Mechanical Engineering, University of Colorado Boulder, Boulder, Colorado, USA.
[2]Department of Atmospheric and Oceanic Sciences, University of Colorado Boulder, Boulder, Colorado, USA.
[3]National Renewable Energy Laboratory, Golden, Colorado, USA.

E-mail: misa5952@colorado.edu

Abstract. Direction and speed wind shear modify turbine performance by changing inflow conditions on turbine blades. Using observations from the 2013 CWEX campaign, we found the daily atmospheric boundary layer transitions (morning and evening) match periods of high electricity demand for a wind farm in central Iowa. Power production during these periods was undermined for large direction shear and low speed shear scenarios. The morning transition displayed larger direction shear over the rotor layer for most wind speeds compared to the evening period. This resulted in lower turbine performance for the morning compared to the evening and whole day. This study shows that the combined effect of direction and speed shear is affecting turbine operation during high electricity demand times of day, predominantly during the morning at this wind farm.

1. Introduction

Wind power generation directly depends on numerous atmospheric conditions. Stability, turbulence, and speed and direction shear have been found to influence turbine performance [1–8]. Ideally, the power extracted by a wind turbine depends on the blade design and the available power flux through the disk swept by the blades [9]. Still, the way in which the available power flux and the blade element's efficiency varies depend on numerous variables, most of which are difficult and require numerous instruments to characterize.

Static stability in the boundary layer is driven by temperature gradients that create or suppress buoyancy [10]. Three distinct stability regimes are usually considered in the boundary layer. Stable atmospheric conditions correspond to net vertical heat fluxes toward the ground that pose a counteracting buoyant force to vertically-moving air parcels. Unstable conditions, in the opposite, present positive vertical heat fluxes at the surface resulting in convective motions of air plumes. Lastly, neutral stability is characterized by near-zero buoyancy and sometimes large mechanical turbulence. Unstable conditions usually dominate during daytime. When solar radiation heats the surface, the boundary layer gets highly mixed and a uniform mean virtual potential temperature profile develops due to convection. During nighttime, a stratified condition prevails. When the surface is colder than the air, turbulent buoyant fluxes cease, and the mean potential temperature increases with height.

Without considering advection or topography, stability in the boundary layer largely determines the evolution of wind speed, wind direction and turbulence across the boundary layer. Highly stable layers

have large vertical shear due to little vertical mixing, and turbulence is mechanically generated [10]. Conversely, vertical momentum fluxes in mixed layers reduce vertical shear but increases turbulence as large convective eddies carry vertical momentum across the layer [10].

Many studies have focused on the effects of the different atmospheric states and variables on wind power generation. Turbulence intensity and wind shear have been found to influence turbine performance [1–4,7]. Atmospheric stability has been linked to deviations from the manufacturer's power curve [5,8,11]. And large direction wind shear has been linked to slight decreases of turbine power production [4,12].

Most of the studies mentioned above focus on the effect of atmospheric conditions on turbine performance during a stationary atmospheric regime, however the transition periods between nighttime and daytime and vice-versa are rarely considered. After sunrise, a stratified boundary layer evolves to well-mixed, and near sunset the opposite transpires. Studies on the evening transition have centered on the convective-to-nocturnal boundary layer evolution [13–18], the vertical transport of species [19,20] and the evolution of low-level jets [21–24]. In addition, its effects on wind turbines such as loads on blades [25] and the evolution of wakes [26,27] have also been considered. Most studies for the morning transition have focused on the evolution from a stable to convective boundary layer and on the definition of the transition period [18,28–32]. The morning and evening transitions are of great importance as they take place during high-demand electricity times of day for the Midwest region of the United States [33]. The morning transition exhibits the largest rate of increase in electricity demand. The evening transition usually initiates just after a maximum in daily electricity demand.

In this study, we investigate the influence of speed and direction wind shear on turbine performance during the morning and evening transition periods. In addition, we intend to verify if the threshold defined by Sanchez Gomez and Lundquist [34] is able to discern between under- and overperformance for different boundary layer structures. Section 2 provides a brief description of the dataset used for this study. In section 3, we present our data analysis methods, including the definition of the morning and evening transitions, and how we characterize direction and speed shear. A characterization of atmospheric states and the effects of each shear condition on turbine performance for each period of the day are highlighted in sections 4 and 5.

2. Data

2.1. Site description

The Crop Wind Energy eXperiment (CWEX) in 2010, 2011 and 2013 intended to study the effect of wind turbines on microclimates over crops [35–37], the diurnal cycle effect on turbine wakes [27,38], and how agriculture impacts wind energy production [39]. Observations during this period have also been used to further analyse the impacts of different atmospheric conditions on turbine power production [24], the dynamics of wake variability [40,41], and to test approaches for coupling mesoscale and large-eddy simulation models [42]. The CWEX campaign of 2013 took place between June and September in a wind farm in north-central Iowa. Several surface flux stations, a radiometer, three profiling lidar, and a scanning lidar were deployed.

Table 1. Technical specifications of the GE 1.5 MW extra-long extended (XLE) model turbines [43].

Rotor diameter (D)	82.5 m
Hub height	80 m
Rated power	1.5 MW
Cut-in wind speed	3.5 m s^{-1}
Rated power at	11.5 m s^{-1}
Cut-out wind speed	20 m s^{-1}

This multi-MW wind farm is composed of 200 wind turbines arranged from the southeast to northwest. The wind farm is layout over flat terrain surrounded by wetlands, a mixture of corn and soybeans, and some farmsteads in the southern edge [35]. A subset of GE 1.5 MW XLE model turbines (see Table 1 for specifications) is used for analysis for the 2013 campaign, from which four turbines are selected for this analysis (see Sanchez Gomez and Lundquist [34] for complete site description). The four turbines for this analysis are selected due to their proximity to the WindCube V1 profiling lidar.

2.2. Profiling lidar

Data from a Leosphere Windcube V1 profiling lidar is used to quantify wind speed, and direction over the turbine rotor layer. This Doppler wind lidar measures vertical profiles of speed and direction at nominally 1-Hz temporal resolution. It uses a Doppler beam swinging (DBS) approach obtaining radial wind measurements along four cardinal directions at an inclination of 62.5º above the horizon [24]. The components of the flow are then calculated from the four separate line-of-sight velocities [44]. The CWEX-13 campaign collected wind measurements from 40 to 220 m above ground level (AGL) at 20 m increments. This study focuses on 2-min average measurements from 40 to 120 m, which comprise the entire turbine rotor layer.

Lidar and turbine data is available throughout the campaign [34]. The prevailing wind direction is from the south. Additionally, the same procedure as in Sanchez Gomez and Lundquist [34] is followed to filter out wind speeds outside cut-in and rated, and directions <100 and >280 deg so that the lidar captures turbine's inflow conditions.

2.3. Wind turbines

The subset of turbines employed for this study consists of four GE 1.5 MW XLE, variable speed and variable blade pitch turbines. Turbine power production, blade pitch angles and nacelle wind speed were provided by the wind farm operator as 10-min averages recorded through the supervisory control and data acquisition (SCADA) system for each turbine. Turbine operation was filtered following the blade pitch angle approach of St. Martin et al. [5] as depicted in Sanchez Gomez and Lundquist [34].

3. Methods

3.1. Morning and evening transitions

The atmospheric boundary layer undergoes two transitional periods during the day defined by the balance of surface sensible heat fluxes. The morning transition period begins when the surface sensible heat flux becomes positive, causing the shallow nocturnal mixed layer to grow into the residual layer. The evening transition begins with a negative surface sensible heat flux that drives the decay of convective turbulence. Different methodologies have been employed to characterize daily transition periods. Sandeep et al. [16] characterized one transitive period using the rate of decrease of surface temperature, the rate of change of water vapor mixing ratio, wind variance, temperature gradients, signal-to-noise ratio and the Doppler spectral width. Grimsdell and Angevine [45] described the ending of the daytime convective layer using wind profiler reflectivity and Doppler spectral width. The evening transition period has also been defined according to atmospheric stability shifts and changes in the surface sensible heat flux sign [27,46,47]. Here, we use data from seven surface flux stations between August 23 and September 01, 2013 to define 3-hr morning and evening transition periods that follow the mean kinematic heat flux evolution (Figure 1a).

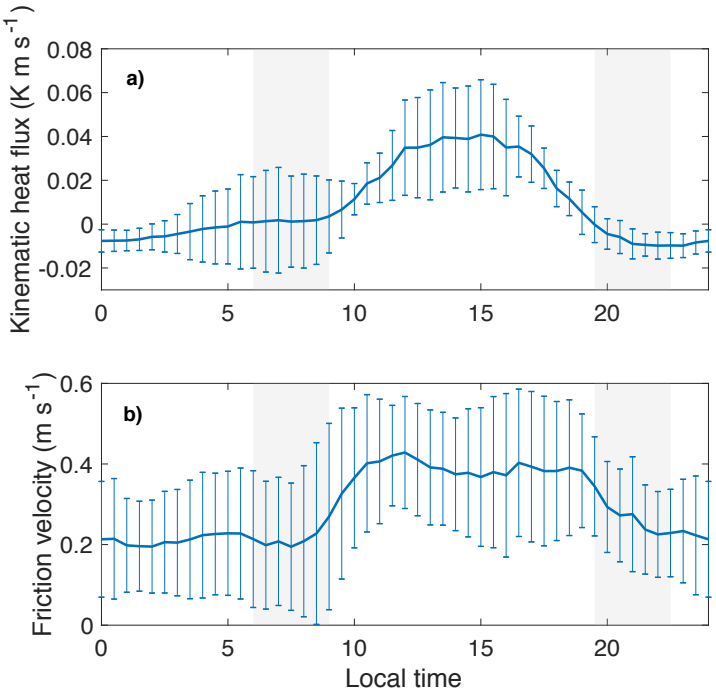

Figure 1. Mean kinematic heat flux (a) and friction velocity (b) evolution from August 23, 2013 to September 01, 2013. Data recorded at 8 m height above ground level. The morning and evening transition periods are shaded in grey on each plot.

After a stable nocturnal layer, the progression of the kinematic heat flux in the surface toward positive values (0600 – 0900 LT) renders an increase of vertical turbulent fluxes (Figure 1b) eroding the stable layer from below. The turbulent eddies increase in size and start to form a mixed layer near the surface. As soon as the convective layer erodes the entire stable layer, it progresses rapidly through the residual neutrally stratified atmosphere.

After a mixed boundary layer developed during the day, vertical turbulent fluxes from the surface are suppressed during the evening transition (1930 – 2230 LT) by a net sensible heat flux toward the ground (Figure 1a). As air cools near the surface, a stratified layer that progresses with height is generated that eventually includes the turbine rotor. The stable layer is characterized by declining vertical momentum fluxes (Figure 1b) that allow winds aloft to increase their speed and start turning clockwise.

3.2. Daily power demand for the Midwest region

Daily power demand in the Midwest region (Figure 2), which includes the state of Iowa, illustrates that the morning transition agrees with the period of largest rate of increase in electricity demand (370 MW hr^{-1}), while the evening transition occurs after the maximum demand period of the day (10 156 MW).

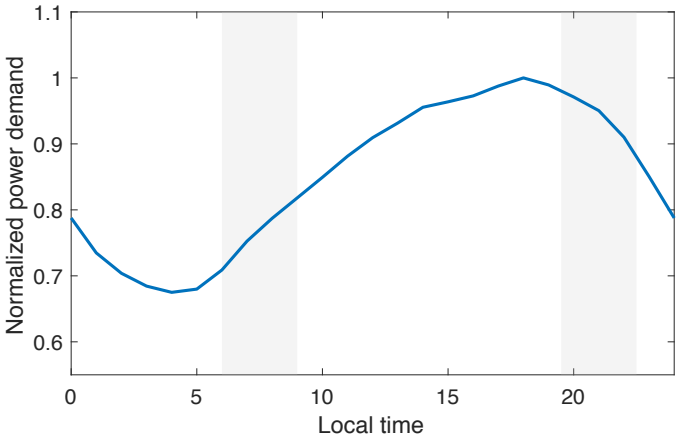

Figure 2. Daily mean power curve for the Midwest region between June and September [33]. The morning and evening transition periods are shaded in grey.

3.3. Normalized performance

Turbine performance throughout the campaign displayed significant differences from the manufacturer's reference values for a wide range of wind speeds [34]. Therefore, the mean power curves obtained for each turbine by Sanchez Gomez and Lundquist [34] were used to normalize power production for each 0.5 m s^{-1} wind speed range. This procedure permits the comparison between different turbines and diverse wind speeds as it establishes performance compared to mean operation during the observed period, where >1 equates turbine overperformance and <1 underperformance.

3.4. Direction wind shear

Direction wind shear corresponds to the change in wind direction with height. Direction shear can be caused by the thermal wind, the inertial oscillation during nighttime [21,23] and frictional drag with the ground. The thermal wind is the vertical shear of geostrophic wind generated by sloping terrain, fronts, lad-sea interfaces, and large-scale weather patterns [10]. The inertial oscillation is the rotation of the wind vector in the boundary layer caused by a force imbalance after short-wave radiation from the sun diminishes around sunset. Friction with the ground reduces the wind speed at the surface and induces a force imbalance between the Coriolis force and pressure gradients, resulting in a surface wind vector crossing isobars toward low pressure [48].

In this study, direction shear is calculated as the shortest rotational path between wind vectors at 40 and 120 m AGL, normalized over the vertical distance between measurements.

3.5. Speed wind shear

Speed shear is defined as the variation of the mean horizontal wind speed with height. Wind speed shear in the atmospheric boundary layer is caused by frictional drag on the air flowing over the surface driven by geostrophic wind. As with direction shear, the forcing mechanisms of speed shear may be thermal winds, the inertial oscillation and friction with the ground [12], as well as other patterns. The short-term variation in wind speed with elevation over shallow layers of the boundary layer is influenced by atmospheric stability. A stable (stratified) layer allows for large speed gradients to develop since buoyant turbulent fluxes are negative and the only contribution to turbulence is shear [10]. An unstable (mixed) layer presents large buoyant turbulent fluxes that carry momentum across the whole layer in addition to shear turbulence generation, resulting in small speed shear [10].

Speed shear in wind energy applications is usually described by the dimensionless wind shear exponent α using the power law expression,

$$V = V_R \left(\frac{z}{z_R}\right)^{\alpha} \quad (1)$$

where V is the mean horizontal wind speed at height z, and V_R is the mean horizontal wind speed at reference height $z_R < z$ above ground level. In this study, we characterize speed shear using the power law and calculate the dimensionless shear exponent using lidar-measured wind speeds at 40 and 120 m AGL.

4. Results

4.1. Atmospheric conditions

The morning transition period during this campaign evidenced a skewed directional shear distribution towards veering, and a skew distribution for speed shear towards large values of the power law exponent (Figure 3). Almost 92% of all recorded cases correspond to wind veering, from which 42% are above 0.2 deg m^{-1}; and for the remaining backing cases, 26% have a numerical value smaller than -0.1 deg m^{-1}. Similarly, more than 94% of cases displayed an increase in wind speed with height, and 45.2% of observations evidenced power law exponents above 0.35, which could cause an 8 m s^{-1} wind speed at the bottom of the rotor layer (40 m) to be up to 12 m s^{-1} at 120 m AGL.

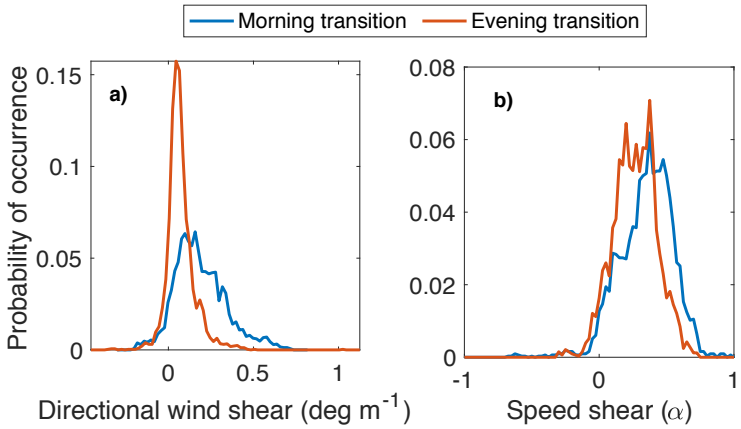

Figure 3. Direction (a) and speed shear (b) distributions for the morning and evening transition over the whole rotor layer.

The evening transition period for the recorded data also presents skewed distributions for direction and speed shear; however, values are closer to zero-shear in both cases (Figure 3). Though 90% of cases correspond to wind veering, only 31% of these have veering values larger than 0.1 deg m^{-1}. Also, only 12.7% of backing cases have numerical values larger than 0.1 deg m^{-1}. Speed shear displays the same trend, as 91.8% of observations have increasing wind speed with height, though the morning transition depicted more cases above $\alpha = 0.35$ given that only 24% of positive power law exponents meet this condition during the evening.

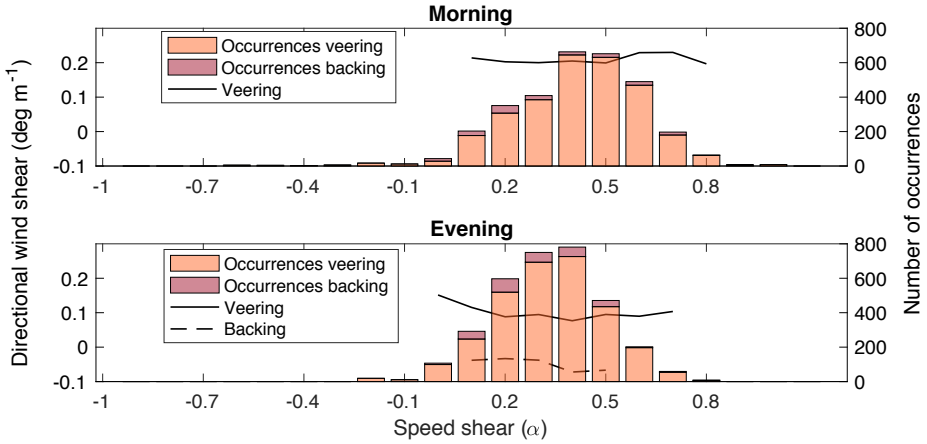

Figure 4. Relationship speed and direction shear for each analyzed time period overlaying the number of occurrences of each direction and speed shear range combination.

Though speed and direction shear depict similar probability distributions and evolution with height, only a minor relationship occurs between these parameters. If only considering mean direction shear values with more than 30 occurrences to approximate a normal distribution for each speed shear bin (Figure 4), an increasing power law exponent value is related to a near-constant directional wind shear for both time periods. The morning transition displays a relationship of 0.37 per unit increase in deg m^{-1} between speed shear and veering for power law exponents larger than 0, however the correlation between veering and α is not significant ($\rho = 0.2132$, $p = 0.61$). Not enough backing cases occurred to draw conclusions. For the evening transition, a 0.24 increase in the power law exponent per unit increase in deg m^{-1} for veering ($\alpha >$ -0.1) and backing ($\alpha > 0$) is observed. Still, no significant linear correlation exists between both shear parameters ($\rho = -0.5833$, $p = 0.13$ for veering; $\rho = -0.5291$, $p = 0.28$ for backing).

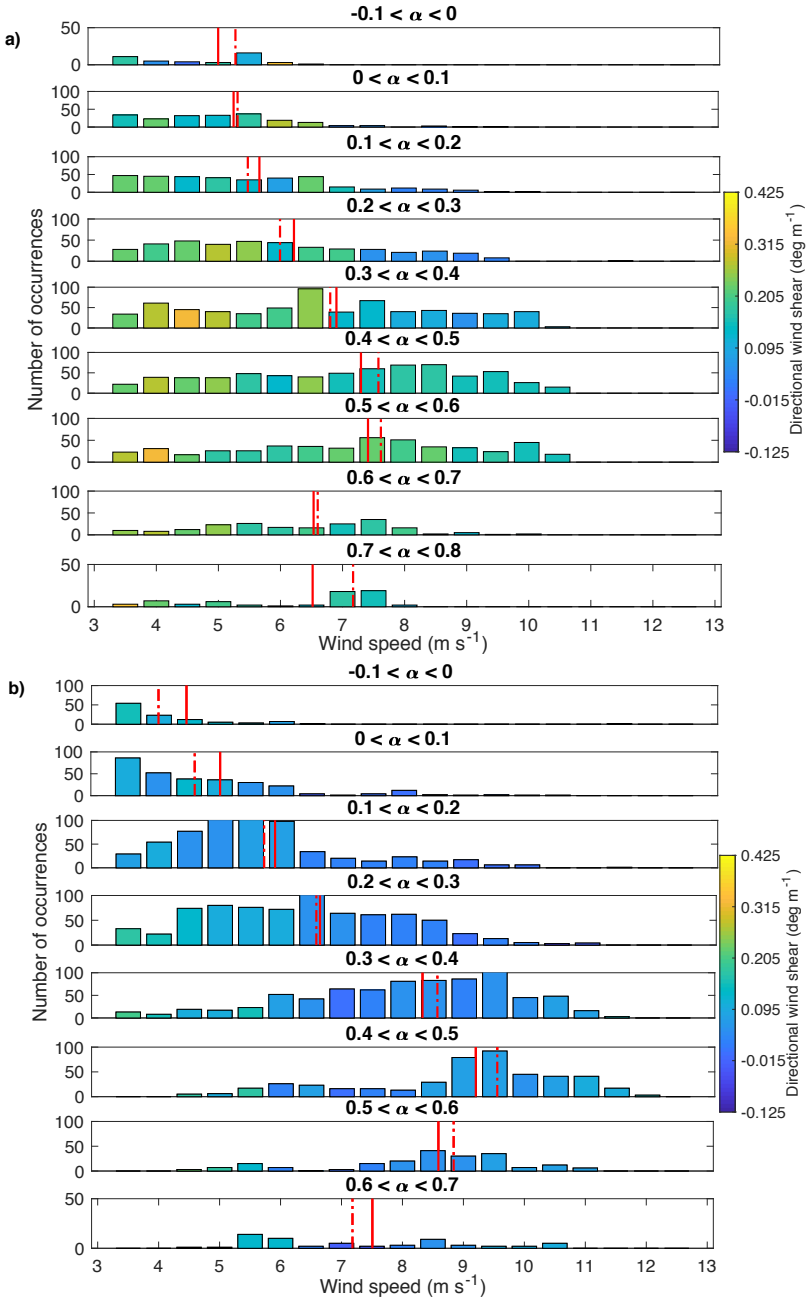

Figure 5. Evolution of speed shear for increasing wind speeds during the morning (a) and evening (b) transitions. Power law bins with more than 30 total observations are plotted. Mean and median wind speeds for each speed shear bin are plotted as continuous and dashed lines, respectively.

The morning transition period portrays greater direction and speed wind shear compared to the evening transition for wind speeds between cut-in and rated speed (Figure 5). The mean wind speed in each speed shear bin follows the same trend for both time periods, with the maxima occurring for $0.5 < \alpha < 0.6$ and $0.4 < \alpha < 0.5$, for the morning and evening transition respectively. However, the morning transition period displays larger direction shear values than the evening transition for every power law exponent and wind speed. More than 37% of observations during the morning evidenced direction shear above 0.2 deg m^{-1} and $\alpha > 0.3$. For the evening, only 0.49% of recordings were above those values, and 17% occurred above $\alpha = 0.3$ and 0.1 deg m^{-1} of directional shear. Furthermore, almost 50% of observations after sunrise having speed and direction shear above $\alpha = 0.3$ and 0.2 deg

m^{-1}, respectively, report wind speeds above 6 m s^{-1}. Conversely, 75% of reported cases near sunset displaying speed shear above $\alpha = 0.3$ and direction shear above 0.1 deg m^{-1} are for speeds below 6 m s^{-1}.

4.2. Turbine performance

Atmospheric conditions during the evening are less unfavorable for turbine power production than during the morning transition (Figure 6). Following the procedure of Sanchez Gomez and Lundquist [34], we segregated normalized performance according to the direction and speed shear conditions at which it took place using a threshold (called the α/β threshold). The α/β threshold corresponds to the combination of speed (α) and direction shear (β) values that separated under- and overperformance at this windfarm [34]. The mean normalized power for the four analyzed turbines for cases above the α/β threshold is 0.88 (a 12% underperformance), while a mean of 1.01 (a 1 % overperformance) occurs for cases below the α/β threshold during the morning transition period [34]. A significance test revealed meaningful differences between normalized power above and below the threshold (99.99% confidence). During the evening transition, mean normalized power for the four analyzed turbines above the α/β threshold is 0.96, and below the threshold is 1, and, as with the morning transition, cases below and above the threshold significantly differ (99.99% confidence). Analyzing each individual turbine yields comparable results to combining them all together.

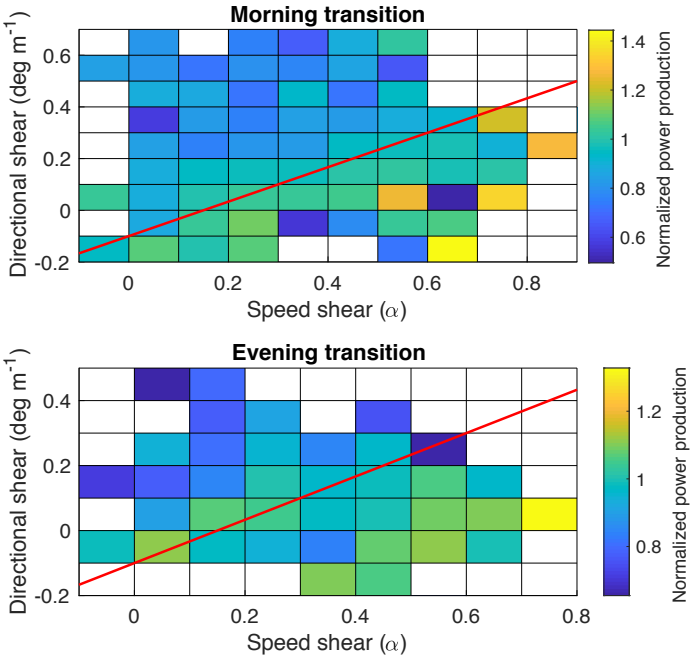

Figure 6. Mean normalized turbine performance for each combination of speed and direction shear values during the morning and evening transitions. The red line marks the α/β threshold. Data for the four analyzed wind turbines.

Examining the factors that influence normalized performance for each turbine reveals that direction shear, as well as speed shear, significantly affects performance in most cases. A multiway analysis of variance on normalized power production for all combinations of speed and direction shear during the morning and evening transitions revealed that direction and speed shear influence normalized power in every turbine (99% confidence).

5. Discussion and conclusions

Wind direction shear during both transition periods evidenced more veering than backing cases (Figure 3), as is expected from the balance between the Coriolis, pressure gradient, and friction forces in the atmospheric boundary layer [10,48]. The evolution of a stable to convective layer during the morning transition causes the newly formed mixed layer to direct the wind vector across isobars

toward low pressure near the surface, while winds upward keep turning in a clockwise manner. For the evening, a stratified layer evolves from a convective lower atmosphere allowing wind vectors aloft to veer.

The morning transition reports more cases and larger values of direction and speed shear than the evening for all wind speeds between cut-in and rated speed (Figure 3 and Figure 5), due to the nature of the evolution from a stratified to convective boundary layer compared to the evolution from convective to stratified. Atmospheric conditions before the morning transition correspond to large shear characteristic of a stratified nocturnal layer. After sunrise, turbulent buoyant fluxes form a mixed layer, however, winds upward are still stratified given that turbulence is yet to be driven by buoyant processes. Observations of the low-level jet in 2013 at this wind farm evidence a predominance of intense jets (LLJ-3) during the morning transition, which report very large speed and direction shear values [24]. After daytime, atmospheric conditions correspond to low direction and speed shear and the buoyancy term in the turbulence budget equation becomes negative. The stratified layer that evolves near the surface allows for shear to develop. However, mechanical turbulence in the residual layer above is large, mimicking former atmospheric conditions, hindering shear evolution. Low-level jets during the evening are generally weaker, of low intensity classes [24]. Near-uniform winds in the mixed layer and residual stratified winds aloft, and a greater incidence of high intensity jets during the morning transition result in large shear over a thinner layer compared to the evening.

Though speed and direction shear in the boundary layer have equivalent forcing mechanisms, they do not display a proportional relationship (Figure 4). Cariou et al. [49] suggests a larger correspondence between speed and direction shear over land, however our results show the opposite for transition periods. The increase of speed and direction shear over the whole rotor layer during each transition period depends on the rate of change of the wind vector (speed and direction) for each height interval, which differs for the morning and evening periods. During the morning transition, frictional forces driven by convection in the lower rotor layer increase rapidly (rapid decrease in wind speed and rate of direction change) resulting in greater proportionality between both shear parameters. Moreover, if conditions favor “free encroachment”, the mixed layer growth will occur at the fastest possible rate [31] supporting greater proportionality between speed and direction shear. Still, inertia from a nocturnal stratified boundary layer causes the upper layer to remain decoupled. During the evening transition, a stratified flow at lower heights dominates and less correspondence persists between both parameters.

The α/β threshold reported by Sanchez Gomez and Lundquist [34] distinguished between under- and overperformance for periods with different boundary layer structures. The morning transition presents an evolving stratified to convective layer comprised of a growing mixed layer near the surface, capped by a stable and residual layer. In contrast, the evening transition corresponds to an evolving mixed to stable layer, composed of a shallow surface layer topped by a growing stable layer beneath a residual/mixed layer. Segregating turbine performance according to speed and direction shear allowed differentiation between detrimental and favorable conditions in both transitive periods.

Substantial veering coupled with small speed shear is related to underperformance, in contrast, large speed shear and small changes in wind direction evidenced a boost in power above the mean for both transitive periods throughout the campaign (Figure 6). The alteration of inflow conditions varies the available power of the air through the turbine and its ability to extract energy from the wind [50]. Similar findings were reported in Ref. [34] when considering the effect of direction and speed shear for the whole day. Model results [4,12] and our observations, however, present opposing findings for constant direction shear and increasing speed shear. The opposite monotonical relationship between performance and speed shear found in both transition periods, and the decrease in the energy flux ($0 < \alpha < 0.33$) and turbine performance in simulations suggests that turbines in this wind farm present dissimilar aerodynamic efficiencies from that in the models, or that additional forcing mechanisms such as varying turbulence may exist in our observations.

Turbine performance during the morning transition differs from than during the evening and reports inferior values. Underperformance was approximately 3 times larger for the morning relative

to the evening transitive period (12% and 4%, respectively). Similarly, power reductions were much larger for the morning transition compared to whole-day results (12% for the morning and 6% for the whole day [34]). The morning transition presented larger direction shear for the majority of wind speeds compared to the evening. Also, greater proportionality between both shear parameters resulted in more power production cases taking place further above from the α/β threshold, in the region of underperformance. Furthermore, the multiway analysis of variance showed that direction shear effectively influenced turbine performance. Therefore, the occurrence of larger wind veer during the morning resulted in lower turbine performance compared to the evening.

Large shear values recorded during both transition periods and the observed power reductions that they instigate make speed and direction shear meaningful when considering atmospheric conditions that influence turbine performance during high power-demanding times of day. The morning transition evidenced more underperformance cases than the evening due to larger speed and direction shear values. However, direction and speed shear for the high power-demand time period is still significant. Therefore, this study shows that the periods with the largest rate of increase and value of power demand in the Midwest region are affected by speed and direction shear. These results are representative for locations with strong diurnal variability and flat terrain. It remains to be seen if the mid-day and mid-night periods are also affected. We speculate that the night period will be the most affected of the two. Also, we recommend verifying if the α/β threshold is still able to discriminate between turbine over- and underperformance at other locations, for different turbines and when including the effects of turbulence.

6. Acknowledgements

The CWEX project was supported by the National Science Foundation under the State of Iowa EPSCoR grant 1101284. The role of the University of Colorado Boulder in CWEX-13 was supported by the National Renewable Energy Laboratory. The authors thank NextEra Energy for providing the wind turbine power data. This work was authored [in part] by the National Renewable Energy Laboratory, operated by Alliance for Sustainable Energy, LLC, for the U.S. Department of Energy (DOE) under Contract No. DE-AC36-08GO28308. Funding provided by the U.S. Department of Energy Office of Energy Efficiency and Renewable Energy Wind Energy Technologies Office. The views expressed in the article do not necessarily represent the views of the DOE or the U.S. Government. The U.S. Government retains and the publisher, by accepting the 5 article for publication, acknowledges that the U.S. Government retains a nonexclusive, paid-up, irrevocable, worldwide license to publish or reproduce the published form of this work, or allow others to do so, for U.S. Government purposes.

7. References

[1] Antoniou I, Pedersen S M and Enevoldsen P B 2009 Wind Shear and Uncertainties in Power Curve Measurement and Wind Resources *Wind Engineering* **33** 449–68

[2] Elliot D L and Cadogan J B 1990 Effects of wind shear and turbulence on wind turbine power curves European Community Wind Energy Conference and Exhibition (Madrid) pp 10–4

[3] Kaiser K, Langreder W, Hohlen H and Højstrup J 2007 Turbulence Correction for Power Curves *Wind Energy* ed J Peinke, P Schaumann and S Barth (Berlin, Heidelberg: Springer Berlin Heidelberg) pp 159–62

[4] Rareshide E, Tindal A, Johnson C, Graves A, Simpson E, Bleeg J, Harris T and Schoborg D 2009 Effects of Complex Wind Regimes on Turbine Performance AWEA WINDPOWER Conference (Chicago) pp 1-15

[5] St. Martin C M, Lundquist J K, Clifton A, Poulos G S and Schreck S J 2016 Wind turbine power production and annual energy production depend on atmospheric stability and turbulence *Wind Energy Science* **1** 221–36

[6] Sumner J and Masson C 2006 Influence of Atmospheric Stability on Wind Turbine Power Performance Curves *Journal of Solar Energy Engineering* **128** 531

[7] Wharton S and Lundquist J K 2012 Atmospheric stability affects wind turbine power collection *Environmental Research Letters* **7** 014005

[8] Wharton S and Lundquist J K 2012 Assessing atmospheric stability and its impacts on rotor-disk wind characteristics at an onshore wind farm: Atmospheric stability on rotor-disk wind characteristics *Wind Energy* **15** 525–46

[9] Burton T, Sharpe D, Jenkins N and Bossanyi E 2001 *Wind energy: handbook* (Chichester ; New York: J. Wiley)

[10] Stull R B 1988 *An introduction to boundary layer meteorology* (Dodrecht: Kluwer Academic Publishers)

[11] Vanderwende B J and Lundquist J K 2012 The modification of wind turbine performance by statistically distinct atmospheric regimes *Environmental Research Letters* **7** 034035

[12] Walter K, Weiss C C, Swift A H P, Chapman J and Kelley N D 2009 Speed and Direction Shear in the Stable Nocturnal Boundary Layer *Journal of Solar Energy Engineering* **131** 011013

[13] van Driel R and Jonker H J J 2011 Convective Boundary Layers Driven by Nonstationary Surface Heat Fluxes *Journal of the Atmospheric Sciences* **68** 727–38

[14] Jensen D D, Nadeau D F, Hoch S W and Pardyjak E R 2016 Observations of Near-Surface Heat-Flux and Temperature Profiles Through the Early Evening Transition over Contrasting Surfaces *Boundary-Layer Meteorology* **159** 567–87

[15] Nadeau D F, Pardyjak E R, Higgins C W, Huwald H and Parlange M B 2013 Flow during the evening transition over steep Alpine slopes *Quarterly Journal of the Royal Meteorological Society* **139** 607–24

[16] Sandeep A, Rao T N and Rao S V B 2015 A comprehensive investigation on afternoon transition of the atmospheric boundary layer over a tropical rural site *Atmospheric Chemistry and Physics* **15** 7605–17

[17] Sorbjan Z 1997 Decay of convective turbulence revisited *Boundary-Layer Meteorology* **82** 503–17

[18] Sorbjan Z 2007 A numerical study of daily transitions in the convective boundary layer *Boundary-Layer Meteorology* **123** 365–83

[19] Angevine W M and Mitchell K 2001 Evaluation of the NCEP Mesoscale Eta Model Convective Boundary Layer for Air Quality Applications *Monthly Weather Review* **129** 2761–75

[20] Sorbjan Z 2003 *Air quality modeling: theories, methodologies, computational techniques, and available databases and software* ([S.l.] : Pittsburgh, PA: EnviroComp ; Air & Waste Management Association)

[21] Blackadar A K 1957 Boundary Layer Wind Maxima and Their Significance for the Growth of Nocturnal Inversions *Bulletin of the American Meteorological Society* **38** 283–90

[22] Mahrt L 2007 The early evening boundary layer transition *Quarterly Journal of the Royal Meteorological Society* **107** 329–43

[23] Van de Wiel B J H, Moene A F, Steeneveld G J, Baas P, Bosveld F C and Holtslag A A M 2010 A Conceptual View on Inertial Oscillations and Nocturnal Low-Level Jets *Journal of the Atmospheric Sciences* **67** 2679–89

[24] Vanderwende B J, Lundquist J K, Rhodes M E, Takle E S and Irvin S L 2015 Observing and Simulating the Summertime Low-Level Jet in Central Iowa *Monthly Weather Review* **143** 2319–36

[25] Lu N, Basu S and Manuel L 2019 On wind turbine loads during the evening transition period *Wind Energy*

[26] Englberger A and Dörnbrack A 2018 Impact of the Diurnal Cycle of the Atmospheric Boundary Layer on Wind-Turbine Wakes: A Numerical Modelling Study *Boundary-Layer Meteorology* **166** 423–48

[27] Lee J C Y and Lundquist J K 2017 Observing and Simulating Wind-Turbine Wakes During the Evening Transition *Boundary-Layer Meteorology* **164** 449–74

[28] Angevine W M, Baltink H K and Bosveld F C 2001 Observations Of The Morning Transition Of The Convective Boundary Layer *Boundary-Layer Meteorology* **101** 209–27

[29] Beare R J 2008 The Role of Shear in the Morning Transition Boundary Layer *Boundary-Layer Meteorology* **129** 395–410

[30] Lapworth A 2006 The Morning Transition of the Nocturnal Boundary Layer *Boundary-Layer Meteorology* **119** 501–26

[31] Sorbjan Z 1996 Effects Caused by Varying the Strength of the Capping Inversion Based on a Large Eddy Simulation Model of the Shear-Free Convective Boundary Layer *Journal of the Atmospheric Sciences* **53** 2015–24

[32] White A B, Templeman B D, Angevine W M, Zamora R J, King C W, Russell C A, Banta R M, Brewer W A and Olszyna K J 2002 Regional contrast in morning transitions observed during the 1999 Southern Oxidants Study Nashville/Middle Tennessee Intensive: REGIONAL CONTRAST IN MORNING TRANSITIONS *Journal of Geophysical Research: Atmospheres* **107** ACL 21-1-ACL 21-12

[33] U.S. Energy Information Administration 2019 *U.S. Electric System Operating Data: Regional electricity demand (Midwest)* (U.S. Energy Information Administration)

[34] Sanchez Gomez M and Lundquist J K 2019 The effect of wind direction shear on turbine performance in a wind farm in central Iowa *Wind Energy Science Discussions* 1–23

[35] Rajewski D A, Takle E S, Lundquist J K, Oncley S, Prueger J H, Horst T W, Rhodes M E, Pfeiffer R, Hatfield J L, Spoth K K and Doorenbos R K 2013 Crop Wind Energy Experiment (CWEX): Observations of Surface-Layer, Boundary Layer, and Mesoscale Interactions with a Wind Farm *Bulletin of the American Meteorological Society* **94** 655–72

[36] Rajewski D A, Takle E S, Lundquist J K, Prueger J H, Pfeiffer R L, Hatfield J L, Spoth K K and Doorenbos R K 2014 Changes in fluxes of heat, H2O, and CO2 caused by a large wind farm *Agricultural and Forest Meteorology* **194** 175–87

[37] Rajewski D A, Takle E S, Prueger J H and Doorenbos R K 2016 Toward understanding the physical link between turbines and microclimate impacts from in situ measurements in a large wind farm: Microclimates with turbines on versus off *Journal of Geophysical Research: Atmospheres* **121** 13,392-13,414

[38] Rhodes M E and Lundquist J K 2013 The Effect of Wind-Turbine Wakes on Summertime US Midwest Atmospheric Wind Profiles as Observed with Ground-Based Doppler Lidar *Boundary-Layer Meteorology* **149** 85–103

[39] Vanderwende B and Lundquist J K 2016 Could Crop Height Affect the Wind Resource at Agriculturally Productive Wind Farm Sites? *Boundary-Layer Meteorology* **158** 409–28

[40] Bodini N, Zardi D and Lundquist J K 2017 Three-dimensional structure of wind turbine wakes as measured by scanning lidar *Atmospheric Measurement Techniques* **10** 2881–96

[41] Lundquist J K, Takle E S, Boquet M, Kosovic B, Rhodes M E, Rajewski D, Doorenbos R, Irvin S, Aitken M L, Friedrich K, Quelet P T, Rana J, Martin C St, Vanderwende B and Worsnop R 2014 Lidar observations of interacting wind turbine wakes in an onshore wind farm *EWEA meeting proceedings* 10–3

[42] Muñoz-Esparza D, Lundquist J K, Sauer J A, Kosović B and Linn R R 2017 Coupled mesoscale-LES modeling of a diurnal cycle during the CWEX-13 field campaign: From weather to boundary-layer eddies: Coupled mesoscale-LES of a diurnal cycle *Journal of Advances in Modeling Earth Systems* **9** 1572–94

[43] General Electric 2009 *GE Energy 1.5MW Wind Turbine*

[44] Lundquist J K, Churchfield M J, Lee S and Clifton A 2015 Quantifying error of lidar and sodar Doppler beam swinging measurements of wind turbine wakes using computational fluid dynamics *Atmospheric Measurement Techniques* **8** 907–20

[45] Grimsdell A W and Angevine W M 2002 Observations of the Afternoon Transition of the Convective Boundary Layer *Journal of Applied Meteorology* **41** 3–11

[46] Acevedo O C and Fitzjarrald D R 2001 The Early Evening Surface-Layer Transition: Temporal and Spatial Variability *Journal of the Atmospheric Sciences* **58** 2650–67

[47] Grant A L M 1997 An observational study of the evening transition boundary-layer *Quarterly Journal of the Royal Meteorological Society* **123** 657–77

[48] Holton J R and Hakim G J 2013 *An introduction to dynamic meteorology* (Amsterdam: Academic Press)

[49] Cariou N, Wagner R and Gottschall J 2010 *Analysis of vertical wind direction and speed gradients for data from the met. mast at Høvsøre* (Roskilde: Risø National Laboratory)

[50] Wagner R, Courtney M, Larsen T J and Schmidt Paulsen U 2010 *Simulation of shear and turbulence impact on wind turbine performance* (Denmark: Danmarks Tekniske Universitet)